# Calculation of Intercavity Coupling Coefficient for Side Coupled Standing Wave Linear Accelerator

Rajat Roy and O. Shanker

*Abstract*— **Expressions are developed for the main to side cavity coupling coefficient of a side coupled standing wave linac structure and for the shift in cavity resonant frequency produced by the coupling iris. The theoretical predictions show reasonable agreement with the measured values.**

## I. Introduction

Our institution fabricates linear accelerator (linac) systems for radiotherapy and radiography. The linac tubes are of the side coupled type [1], [2] and are operated in the standing wave mode at 2998 MHz. Fig. 1 shows the basic cell consisting of two main half-cavities joined by a side cavity. The linac tube is built up by stacking these basic cells to form full main cavities. The microwave coupling between cavities is through the iris hole between the main and side cavities. The value of this coupling coefficient is an important parameter in designing the linac. Till recently we had no access to calculations of this coupling coefficient, and had to rely solely on experimental measurements. We have now managed to develop calculation techniques for the coupling constant, and these techniques form the subject matter of this paper.

The equivalent circuit of two coupled half-cavities is shown in Fig. 2. The microwave field distribution and the mode spectrum resulting from the coupling of several microwave resonant cavities are given in [1]–[5]. These are useful in the experimental measurement of the coupling constant (Section II). [6], [7] discuss the design of the optimum cavity shape. The design process can be greatly simplified if one has a theoretical prediction for the coupling coefficient and the shift in cavity frequency due to the opening of the iris. The techniques for such a prediction are presented in Section III, using the theory of diffraction by small holes developed by Bethe [8], generalized to the case of an elliptical iris. In Section IV we compare the theoretical predictions (using the cavity field values calculated by the FEM [7]) with the experimental results, and present the conclusions.

## II. Experimental Determination of the Coupling Constant

The experimental determination of the intercavity coupling constant is quite straightforward and involves only the measurement of the system resonant frequencies. The frequency measurement is done using the textbook method of displaying the reflection coefficient as a function of frequency using a sweep oscillator and a network analyzer, and finding where the dips in the reflection coefficient occur. These give the resonant frequencies to an accuracy of 0.01 MHz when special care is taken and 0.1 MHz under normal conditions. When one of the cavities is detuned we get one resonant frequency, the resonant frequency of the non-detuned cavity. When neither cavity is detuned we get a pair of frequencies. The shifts of these frequencies from the resonant frequencies of the uncoupled cavities are functions of the coupling coefficient, and thus the coefficient can be determined using the expressions presented in [2]–[5].

Manuscript received June 9, 1992; revised November 9, 1992.
The authors are with S.A.M.E.E.R., I.I.T. Campus, Bombay-400076. India.
IEEE Log Number 9209354.

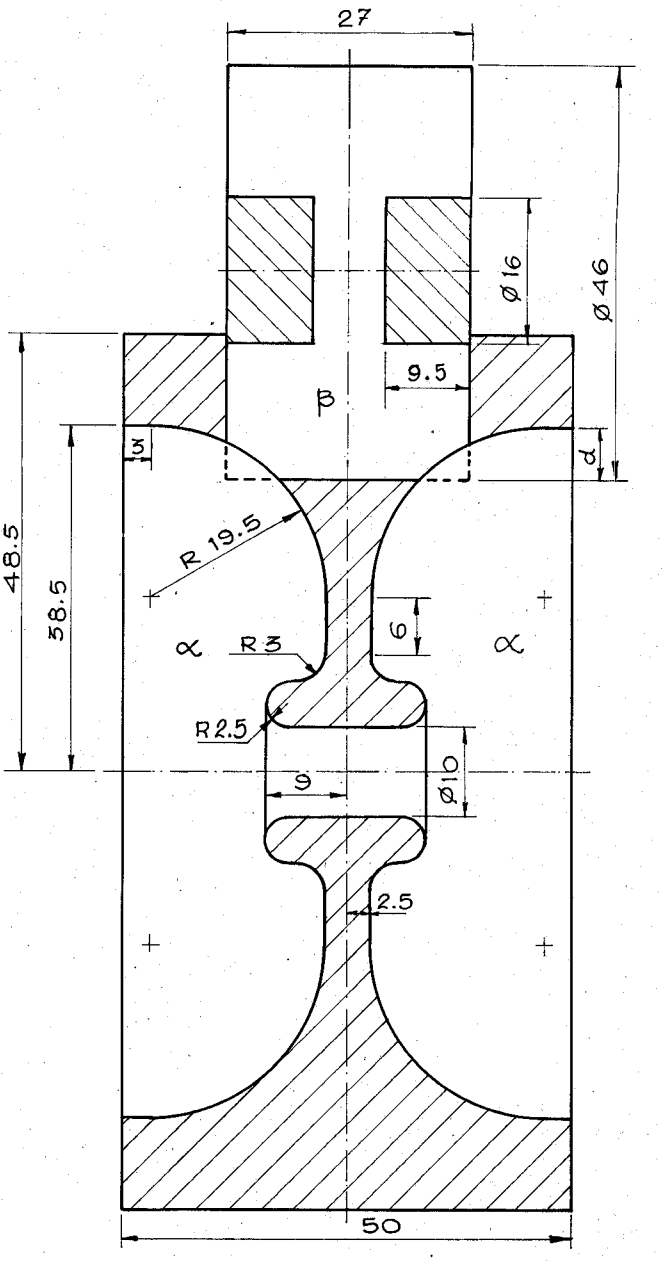


Fig. 1. Main and side cavities (dimensions are in mm).

## III. Theory of Coupled Microwave Cavities

The equations of the coupled modes of oscillations of two cavities with a circular hole in their common wall are given by Bethe [8]. In terms of the cavity excitations $q_\alpha$ and $q_\beta$ and the cavity frequencies $\omega_\alpha$ and $\omega_\beta$, these equations are (Eq. nos. (78) and (78a) of [8])

$$\frac{d^2q_\alpha}{dt^2} + \frac{\omega_0}{Q_\alpha}\frac{dq_\alpha}{dt} + \omega_\alpha^2 q_\alpha = \frac{4}{3}\omega_0^2\frac{a^3}{V_\alpha}(c_{\alpha\alpha}q_\alpha - c_{\alpha\beta}q_\beta)$$
$$\frac{d^2q_\beta}{dt^2} + \frac{\omega_0}{Q_\beta}\frac{dq_\beta}{dt} + \omega_\beta^2 q_\beta = \frac{4}{3}\omega_0^2\frac{a^3}{V_\beta}(c_{\beta\beta}q_\beta - c_{\alpha\beta}q_\alpha), \quad (1)$$

with $c_{ij} = 2\vec{F}_i \cdot \vec{F}_j - \vec{A}_{in} \cdot \vec{A}_{jn}$, and where the subscripts $i$ and $j$ range over the values $\alpha$ and $\beta$ and refer to the two coupled cavities respectively, the subscript $n$ denotes the component normal to the

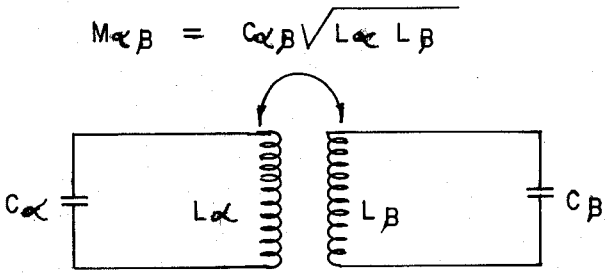


Fig. 2. Equivalent circuit for the cavities, showing the intercavity coupling coefficient represented as a mutual inductance.

aperture (Bethe uses the notation $x$ in place of $n$), $F_m$ are the vector potentials for different mode indices $m$, $A_m$ is curl $F_m/k_m$ and the cavity fields are given in terms of these potentials by

$$\vec{H} = \frac{1}{c}\sum_m \frac{dq_m}{dt}\vec{F}_m(\vec{r})$$

and

$$\vec{E} = \sum_m q_m k_m \vec{A}_m(\vec{r}). \tag{2}$$

The relationship of Bethe's coupling coefficient $c_{\alpha\beta}$ to the mutual inductance $M_{\alpha\beta}$ occurring as a parameter in the equivalent circuit model is given in Fig. 2. In (1) we consider only the lowest mode $(m = 1)$. Also, in all the small quantities involving $c_{\alpha\alpha}$, $c_{\beta\beta}$, $c_{\alpha\beta}$ and the $1/Q_\alpha$ and $1/Q_\beta$ terms we use the average frequency $\omega_0 = (\omega_\alpha + \omega_\beta)/2$ in place of the almost equal frequencies $\omega_\alpha$ and $\omega_\beta$.

The coupled cavity system with two identical half main cavities $\alpha$ and a side cavity $\beta$ is shown in Fig. 1. The shape of the coupling aperture (Fig. 3) between the cavities is quite different from a circle and is furthermore on a curved surface. However one can make a simplifying assumption that the iris is an elliptical one with $l_1$ and $l_2$ as shown in Fig. 3 as its semi-major and semi-minor axes respectively. The assumed centre of the ellipse is the point marked with a cross on the same figure. The generalization of equation (1) for an elliptical hole from a circular one can be easily made following the steps of Collin [9]. Since the actual iris has some sharp corners, the fringing fields near these corners will introduce errors which limit the accuracy of the solution. The errors are small enough for the method to yield useful results.

A further assumption we have to make to apply Bethe's formulation to our problem is that the aperture lies on the common wall of the two coupled cavities. This is not strictly true for our problem as the side cavity and the main cavity volumes overlap each other in the region of the aperture. Thus while we can consider the aperture to be on the wall of the main cavity the side cavity shape has to be perturbed to make the aperture lie on its boundary wall. However if this perturbation is small the field distribution will not substantially change and this is the case when the depth of overlap 'd' shown in Fig. 1 is small.

To evaluate the quantities $c_{\alpha\alpha}$, $c_{\beta\beta}$ and $c_{\alpha\beta}$ we use the fields of the unperturbed side cavity, that is, assuming d to be small which becomes increasingly false at higher values of the coupling between the cavities. The component of the electric field normal to the aperture and of the magnetic field tangential to it have to be evaluated at the interior points of the side cavity because these are the components that enter in the expressions for $c_{\alpha\alpha}$, $c_{\beta\beta}$ and $c_{\alpha\beta}$. For the main cavity side where the aperture lies on its wall this is already taken care of as the total electric field is always normal and the magnetic field always tangential to it.

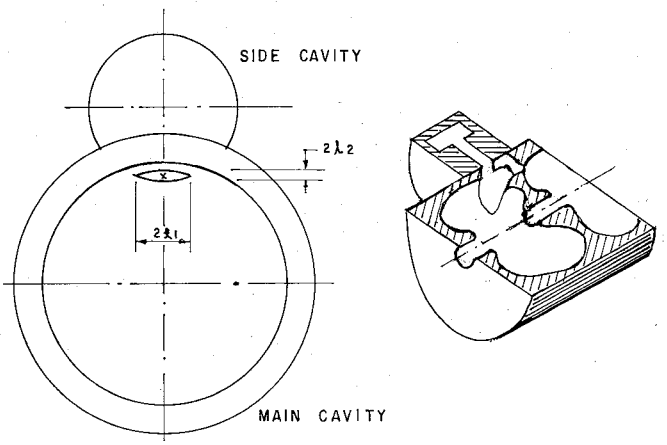


Fig. 3. The aperture shape showing the length of the major and minor axis respectively of the equivalent ellipse by which it is represented. Inset shows an isometric view of the iris and the cavities.

The generalization of equation (1) for an elliptical aperture along with the appropriate alterations introduced to take into account a change from the Gaussian system of units used by Bethe to a MKS system used by Collin [9] gives

$$\begin{aligned}\frac{d^2q_\alpha}{dt^2} + \omega_\alpha^2 q_\alpha &= \omega_0^2(C_{\alpha\alpha}q_\alpha - C_{\alpha\beta}q_\beta)\\ \frac{d^2q_\beta}{dt^2} + \omega_\beta^2 q_\beta &= \omega_0^2(C_{\beta\beta}q_\beta - C_{\alpha\beta}q_\alpha),\end{aligned} \tag{3}$$

where $C_{ij}$ ($i$, $j$ ranging over the values $\alpha$ and $\beta$) is

$$\begin{aligned}C_{ij} = {} & \frac{2\pi l_1^3 e^2}{3[k(e) - E(e)]}\vec{H}_{xi}\cdot\vec{H}_{xj}\\ & + \frac{2\pi l_1^3 e^2(1-e^2)}{3[E(e) - (1-e^2)K(e)]}\vec{H}_{yi}\cdot\vec{H}_{yj}\\ & - \frac{2\pi l_1^3(1-e^2)}{3E(e)}\vec{E}_{ni}\cdot\vec{E}_{nj}\end{aligned} \tag{4}$$

and where the '$E$'s and the '$H$'s are the components of the time independent parts of the dominant mode of the electric and magnetic fields respectively of each cavity ($\alpha$ or $\beta$) normalized according to

$$\int_\alpha \mu_0\left|\vec{H}_\alpha\right|^2 d\tau = \int_{\beta/2} \mu_0\left|\vec{H}_\beta\right|^2 d\tau = 1$$

instead of (65d) of Bethe [8]. In the above, $e$ is the eccentricity of the ellipse, $l_1$ is its semi-major axis and $K(e)$ and $E(e)$ are the complete elliptic integrals of the first and second kind [10]. While evaluating $\vec{H}_{x\alpha}\cdot\vec{H}_{x\beta}$ or $\vec{H}_{y\alpha}\cdot\vec{H}_{y\beta}$ in the expressions for $C_{\alpha\beta}$ one should be careful to take into account the sense of the fields in each cavity. Henceforth we also neglect the loss term assuming '$Q$'s to be infinite as we did in (3). We also note that the upper-case '$C$' has been used in (3) and (4) in place of the lower case letter used for the corresponding quantities in (1) and (2) to maintain a distinction. From (3) we see that a result of cutting the iris, the frequencies of the cavities shift from the uncut values to

$$\omega_\alpha'^2 = \omega_\alpha^2 - \omega_0^2 C_{\alpha\alpha}$$

and

$$\omega_\beta'^2 = \omega_\beta^2 - \omega_0^2 C_{\beta\beta}.$$

The next section gives the application of this theory to calculate the inter-cavity coupling constant and the cavity frequent shift.

TABLE I
COMPARISON OF MEASURED AND CALCULATED PARAMETERS

| Depth of Overlap 'd' (mm) | Main Cavity Frequency (MHz) | | Main to Side Cavity Coupling | |
|---|---|---|---|---|
| | Measured | Calculated | Measured | Calculated |
| 6 | 2997.85 | 2994.96 | 0.0127 | 0.0111 |
| 7.6 | 2991.79 | 2988.16 | 0.0216 | 0.0204 |
| 8.6 | 2987.55 | 2984.69 | 0.0282 | 0.0281 |
| 9.2 | 2984.15 | 2982.94 | 0.0321 | 0.0335 |

## IV. CALCULATIONS AND RESULTS

To evaluate the inter-cavity coupling constant one has to first evaluate the fields at the center of the ellipse by which the aperture is represented. We do this by using the finite element routine developed in [7]. The computed values of the frequency of the main cavity (with the aperture on its wall), and the intercavity coupling constant are given in Table I for different sizes and positions of the iris as determined by the depth of overlap d. Along with these the corresponding experimental values are also given. The uncut resonant frequency of the main cavity used for generating Table I was 3006.7 MHz. Earlier we only had the experimental technique. The new aspect is our ability to predict the values. The prediction is precise enough for our needs during the initial design stage. Thus, we have been able to simplify the design process.

## REFERENCES


[1] D. E. Nagle, E. A. Knapp, and B. C. Knapp, "Coupled resonator model for standing wave accelerator tanks," *Rev. Sci. Instr.*, vol. 38, p. 1583, 1967.

[2] E. A. Knapp, B. C. Knapp, and J. M. Potter, "Standing wave high energy linear accelerator structures," *Rev. Sci. Instr.*, vol. 39, p. 979, 1968.

[3] O. Shanker, P. A. Rai Chowdhuri, and R. Verma, "Coupling coefficient information from the linac mode spectrum," *Rev. Sci. Instr.*, vol. 60, p. 3301, 1989.

[4] O. Shanker, "Matrix analysis of coupled cavity structures," in *Proc. Int. Conf. on Millimeter Waves and Microwaves,* Dehra Dun, India, Dec. 1990, Tata McGraw Hill, New Delhi, p. 620.

[5] ——, "Generalization of linac mode spectrum and fitting procedure," *Rev. Sci. Instr.*, vol. 63, p. 4443, 1992.

[6] H. C. Hoyt, D. D. Simmonds, and W. F. Rich, "Computer designed 805 MHz proton linac cavities," *Rev. Sci. Instr.*, vol. 37, p. 755, 1966.

[7] R. Roy and O. Shanker, "Evaluation of microwave linac cavity field and parameters by the finite element method," *Indian J. Pure and Applied Physics,* vol. 30, p. 207, 1992.

[8] H. A. Bethe, "Theory of diffraction by small holes," *Phys. Rev.*, vol. 66, p. 163, 1944.

[9] R. E. Collin, *Field Theory of Guided Waves.* New York: McGraw-Hill, 1960.

[10] E. Jahnke and F. Emde, *Tables of Functions,* 4th ed., New York: Dover, 1945, p. 58.


# Shape Function Optimization in the Finite Element Analysis of Waveguides

H. E. Hernández-Figueroa and G. Pagiatakis

***Abstract*—In this paper, a novel finite element technique is presented, which can substantially reduce the computational effort required for the analysis of waveguide structures. Demonstrative examples, whose finite element solutions are obtained by combining this technique with two well-known formulations—$E_z - H_z$ and $H$-field—are given.**

## I. INTRODUCTION

A drawback of the finite element method when applied to modal waveguide analysis is the extensive use of computer resources: memory space and time. Although the order of the resulting matrix eigenvalue problem mainly depends on the geometry of the specific structure analyzed, the kind of mesh adopted, and the formulation used, most of these problems demand a large amount of data manipulations. However, substantial reduction of the computational effort can be achieved by taking advantage of the Rayleigh–Ritz Principle (RRP), which is the basis of the $\alpha$-finite element technique [1]–[3]. This technique was first introduced by Laura and co-workers (see [1] and references therein) who used modified basis functions for the bilinear quadrilateral ($Q_1$) elements applied to the *scalar* 2-D Helmholtz equation. In [2], novel basis functions were introduced to deal with the versatile linear triangular ($P_1$) elements, and applied to the *vectorial* $E_z - H_z$ formulation [4]. Also, in that reference, the performances of those two sets of basis functions were compared, and the results showed almost no differences in terms of accuracy. However, as the modified $P_1$ functions provide close analytical expressions for the integrals associated with the elements of the elementary matrices, these functions are much more attractive than the $Q_1$ ones, which instead require the use of numerical integration schemes, and therefore, more CPU time.

In this paper, the $P_1$-$\alpha$-finite element technique is presented, and the conditions for combining with finite element formulations for the analysis of waveguide structures are discussed. Also, the feasibility of such combined approaches is demonstrated by making use of the widely known $E_z - H_z$ and $H$-field [5] formulations, applied to the analysis of hollow and dielectric-loaded metallic waveguides which possess analytical solutions [6].

## II. THE $P_1$-$\alpha$-FINITE ELEMENT TECHNIQUE

This technique, contrary to the common practice of increasing the mesh size or the basis function order, minimizes the discretization error, for a given mesh, by taking advantage of the RRP. According to this principle, the approximate eigenvalues $\lambda_i'$, obtained by solving the resulting matrix eigenvalue problem $Ax = \lambda Bx$, where $A$ and $B$ are Hermitian and $B$ is positive definite, are always upper bounds

Manuscript received August 4, 1992; revised December 7, 1992. This work was supported by the Brazilian Agency CAPES and the State Scholarship Foundation of Greece (IKY).

H. E. Hernández-Figueroa was with the Laser Optics Group, Department of Physics, Imperial College, London, SW7 2BZ, U.K. He is now with the Department of Electronic and Electrical Engineering, University College London, Torrington Place, London WC1E 7JE, U.K.

G. Pagiatakis is with the Department of Electrical Engineering, Imperial College, London, SW7 2AZ, U.K.

IEEE Log Number 9209353.